Clay-Reinforced Epoxy Nanocomposites

Tie Lan and Thomas J. Pinnavaia*

Department of Chemistry and
Center for Fundamental Materials Research
Michigan State University
East Lansing, Michigan 48824

Received July 26, 1994
Revised Manuscript Received September 20, 1994

Hybrid organic–inorganic composites typically exhibit mechanical properties superior to those of their separate components. To optimize the performance properties of these materials, it is usually desirable to disperse the inorganic components in the organic matrix on a nanometer length scale.[1-3] One successful approach to achieving such nanocomposites is the in situ polymerization of metal alkoxides in organic matrices via the sol–gel process. Inorganic components, especially silica, have been formed by the hydrolysis and condensation of a mononuclear precursor, such as tetraethoxysilane (TEOS), in many polymer systems.[4-8] Owing to the loss of volatile byproducts formed in the hydrolysis/condensation reaction, it is difficult to control sample shrinkage after molding. More recently, however, novel nonshrinkage hybrids have been reported.[8]

Smectite clays and other layered inorganic materials that can be broken down into nanoscale building blocks are good alternatives to the sol–gel process for the preparation of organic–inorganic nanocomposites.[9] In general, the polymer–clay composites can be divided into three categories: conventional composites, intercalated nanocomposites, and exfoliated nanocomposites. In a conventional composite, the clay tactoids exist in their original aggregated state with no intercalation of the polymer matrix into the clay. In an intercalated nanocomposite the insertion of polymer into the clay structure occurs in a crystallographically regular fashion, regardless of the clay-to-polymer ratio. An intercalated nanocomposite normally is interlayered by only a few molecular layers of polymer and the properties of the composite typically resemble those of the ceramic host.[10-13] In contrast, in an exfoliated nanocomposite,the individual 10-Å-thick clay layers are separated in a continuous polymer matrix by average distances that depend on loading. Usually, the clay content of an exfoliated clay composite is much lower than that of an intercalated nanocomposite. Consequently, an exfoliated nanocomposite has a monolithic structure with properties related primarily to those of the starting polymer.

The exfoliation of smectite clays provides 10-Å-thick silicate layers with high in-plane bond strength and aspect ratios comparable to those found for fiber-reinforced polymer composites. Exfoliated clay nanocomposites formed between organocation exchanged montmorillonites and thermoplastic nylon-6 have recently been described by Toyota researchers.[14-16] Clay exfoliation in the nylon-6 matrix gave rise to greatly improved mechanical, thermal, and rheological properties, making possible new materials applications of this polymer.[17,18]

Epoxy-exfoliated clay nanocomposites formed from Epon-828 resin and *m*-phenylenediamine as the curing agent have been prepared in our laboratory using long-chain alkylammonium-exchanged smectite clays.[19,20] The mechanical properties of the exfoliated nanocomposites, however, were only marginally improved relative to conventional composites. Due to the high glass transition temperature (~150 °C) of the epoxy matrix, the composites were in a glassy state at room temperature. Greatly enhanced properties might be expected for epoxy-exfoliated clay nanocomposites with subambient glass transition temperatures. Thus, it was of interest to us to examine the properties of an epoxy–clay nanocomposite in a rubbery state. In the present work, we report the synthesis and mechanical properties of such composite materials.

Homoionic $CH_3(CH_2)_{n-1}NH_3^+$ montmorillonites, where n = 8, 12, and 18 were prepared from Na^+–montmorillonite (CEC = 92 mequiv/100 g) by ion-exchange reaction with alkylammonium chloride or bromide salts in H_2O/EtOH solution.[21,22] The epoxide resin selected for this work was the diglycidyl ether of bisphenol A (Epon-828, Shell):

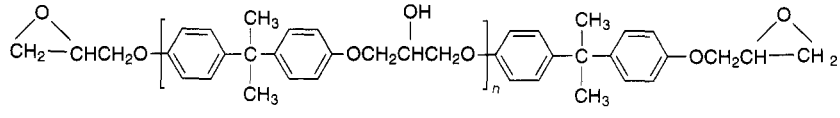

n = 0 (88%); n = 1 (10%); n = 2 (2%)

(1) Giannelis, E. P. JOM **1992**, *44*, 28.
(2) Gleiter, H. *Adv. Mater.* **1992**, *4*, 474.
(3) Novak, B. M. *Adv. Mater.* **1993**, *5*, 422.
(4) Philipp, G.; Schimdt, H. *J. Non-Cryst. Solids* **1984**, *80*, 283.
(5) Philipp, G.; Schimdt, H. *J. Non-Cryst. Solids* **1986**, *82*, 31.
(6) Wang, S.; Ahmad, Z.; Mark, J. E. *Proc. ACS, Div. Polym. Mater. Sci. Eng. (PMSE)* **1994**, *70*, 305.
(7) Kakimoto, M.; Iyoku, Y.; Morikawa, A.; Yamaguchi, H.; Imai, Y. *Poly. Prepr.* **1994**, *35-1*, 393.
(8) Ellsworth, M. W.; Novak, B. M. *Chem. Mater.* **1993**, *5*, 839.
(9) Pinnavaia, T. J. *Science* **1983**, *220*, 365.
(10) Kato, C.; Kuroda, K.; Misawa, M. *Clays Clay Miner.* **1979**, *27*, 129.
(11) Sugahara, Y.; Sugiyama, T.; Nagayama, T.; Kuroda, K.; Kato, C. *J. Ceram. Soc. Jpn.* **1992**, *100*, 413.
(12) Vaia, R. A.; Ishii, H.; Giannelis, E. P. *Chem. Mater.* **1993**, *5*, 1694.
(13) Messersmith, P. B.; Giannelis, E. P. *Chem. Mater.* **1993**, *5*, 1064.
(14) Fukushima, Y.; Inagaki, S. *J. Inclusion Phenom.* **1987**, *5*, 473.
(15) Fukushima, Y.; Okada, A.; Kawasumi, M.; Kurauchi, T.; Kamigaito, O. *Clay Miner.* **1988**, *23*, 27.
(16) Usuki, A.; Kawasumi, M.; Kojima, Y.; Okada, A.; Kurauchi, T.; Kamingaito, O. *J. Mater. Res.* **1993**, *8*, 1174.
(17) Usuki, A.; Kojima, Y.; Kawasumi, M.; Okada, A.; Fukushima, Y.; Kurauchi, T.; Kamigaito, O. *J. Mater. Res.* **1993**, 8, 1179.
(18) Kojima, Y.; Usuki, A.; Kawasumi, M.; Okada, A.; Fukushima, Y.; Kurauchi, T.; Kamigaito, O. *J. Mater. Res.* **1993**, *8*, 1185.
(19) Lan, T.; Kaviratna, P. D.; Pinnavaia, T. J. *Proc. ACS, Div. Polym. Mater. Sci. Eng. (PMSE)* **1994**, *71*, 528.
(20) Lan, T.; Kaviratna, P. D.; Pinnavaia, T. J., manuscript in preparation.
(21) Lin, C.-L.; Lee, T.; Pinnavaia, T. J. *ACS Symp. Ser.* **1992**, *499*, 145.
(22) Lee, T. Ph.D. Thesis, Michigan State University, 1992.

0897-4756/94/2806-2216$04.50/0

The following poly(ether amine) (JEFFAMINE D2000, Texaco) was used as the curing agent to achieve sub-ambient glass transition temperatures:

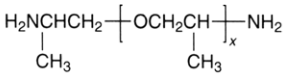

where $x = 33.1$ and the molecular weight is 2000.

Equivalent amounts of the epoxide resin (27.5 wt %) and the polyetheramine (72.5 wt %) were mixed at 75 °C for 30 min. The desired amount of organoclay, from 2 to 23.2 wt %, was added to the epoxide−amine mixture and stirred for another 30 min. The clay−epoxide−amine complex was then outgassed in vacuum for 10 min and transferred into an aluminum mold for curing at 75 °C for 3 h and then at 125 °C for an additional 3 h.

The X-ray diffraction patterns of the epoxy−clay composites containing $CH_3(CH_2)_7NH_3^+-$ and $CH_3(CH_2)_{17}NH_3^+-$montmorillonite are shown in Figure 1. These diffraction patterns reveal the change in clay basal spacing that occurs in the epoxy curing process. It is noteworthy that $CH_3(CH_2)_7NH_3^+-$ and $CH_3(CH_2)_{17}NH_3^+-$montmorillonites respond differently to the epoxide−poly(ether amine) reaction mixture. For $CH_3(CH_2)_7NH_3^+-$montmorillonite (cf. Figure 1A), the initial basal spacing at 15.2 Å is retained throughout the curing process, but significant broadening and reduction of scattering intensity occur for this reflection at 125 °C. For $CH_3(CH_2)_{17}NH_3^+-$montmorillonite (cf. Figure 1B), the basal spacing increases with reaction time and temperature. A new diffraction line with basal spacing at 54 Å appears after curing at 75 °C for 3 h, while the intensity of the original clay diffraction line decreases. With further curing at 125 °C, the clay diffraction lines are too broad to be distinguishable. Therefore, for $CH_3(CH_2)_{17}NH_3^+-$montmorillonite, an exfoliated nanocomposite is achieved. In contrast, $CH_3(CH_2)_7NH_3^+-$montmorillonite is only partially exfoliated in the polymer matrix.

The formation of exfoliated clay nanocomposites is dependent on the nature of the alkylammonium-exchanged clays. Longer linear alkyl chains facilitate the formation of the nanocomposite. Heating the $CH_3(CH_2)_{17}NH_3^+-$montmorillonite system at 75 °C causes the epoxide and amine to migrate into the clay galleries and form an intermediate with a 54 Å basal spacing. Upon additional heating, further polymerization is catalyzed by the acidic primary amine[23−25] and more epoxide and amine enter the galleries, leading to the formation of an exfoliated nanocomposite. Thus, the exfoliation of the clay is caused by intragallery polymer formation. In the case of $CH_3(CH_2)_7NH_3^+-$montmorillonite, the hydrophobicity of the galleries is relatively low, and the amount of intercalated epoxide and amine is insufficient to achieve exfoliation. Therefore, only a portion of the clay is delaminated, as evidenced by the broadening and decreased scattering intensity of the

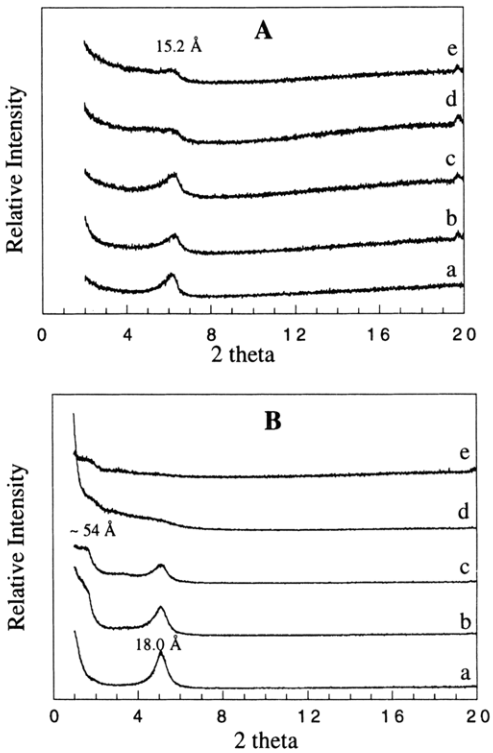

Figure 1. X-ray diffraction patterns of (A) $CH_3(CH_2)_7NH_3^+-$montmorillonite and (B) $CH_3(CH_2)_{17}NH_3^+-$montmorillonite in stoichiometric mixtures of epoxide resin and polyetheramine curing agent after reaction under the following conditions: (a) 75 °C, 10 min; (b) 75 °C, 1 h; (c) 75 °C, 3 h; (d) 75 °C, 3 h and 125 °C, 1 h; (e) 75 °C, 3 h and 125 °C, 3 h. The clay loading in each case was 10 wt %.

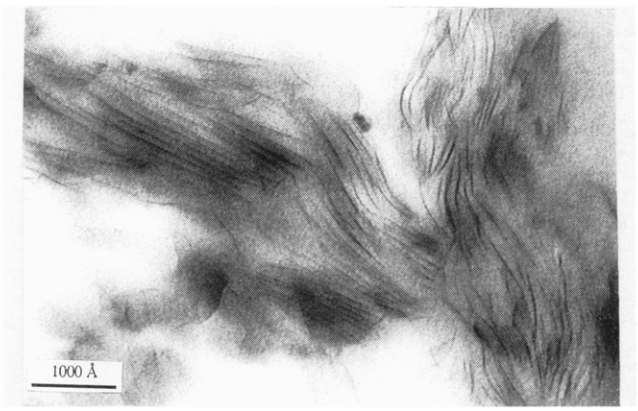

Figure 2. TEM image of an epoxy-clay composite containing 20 wt % $CH_3(CH_2)_{17}NH_3^+-$montmorillonite.

15.2 Å reflection, and the remainder of the clay retains its original basal spacing. Consequently, the final product in the case of $CH_3(CH_2)_7NH_3^+-$montmorillonite is a mixture of exfoliated and conventional clay composites.

A typical TEM image of the epoxy-exfoliated clay nanocomposite containing $CH_3(CH_2)_{17}NH_3^+-$montmorillonite is shown in Figure 2. The dark lines are the cross sections of the 10-Å-thick silicate layers. A face−face layer morphology is retained, but the layers are irregularly separated by ~80−150 Å of polymer. This clay particle morphology is correlated with the absence of Bragg X-ray scattering. The TEM images and XRD patterns of the epoxy composite formed with $CH_3(CH_2)_{11}NH_3^+-$montmorillonite were essentially the same as those for the $CH_3(CH_2)_{17}NH_3^+-$montmorillonite system.

(23) Kamon, T.; Furakaw, H. In *Epoxy Resins and Composites IV*; Dusek, K., Ed. Springer-Verlag: Berlin, 1986; *Advances in Polymer Science*, Vol. 80, p 177.

(24) Barton, J. M. In *Epoxy Resins and Composites I*; Dusek, K., Ed.; Springer-Verlag: Berlin, 1985, *Advances in Polymer Science*, Vol. 72, p 120.

(25) May, C. A., Ed. *Epoxy Resins*, 2nd ed.; Marcel Dekker: New York, 1988.

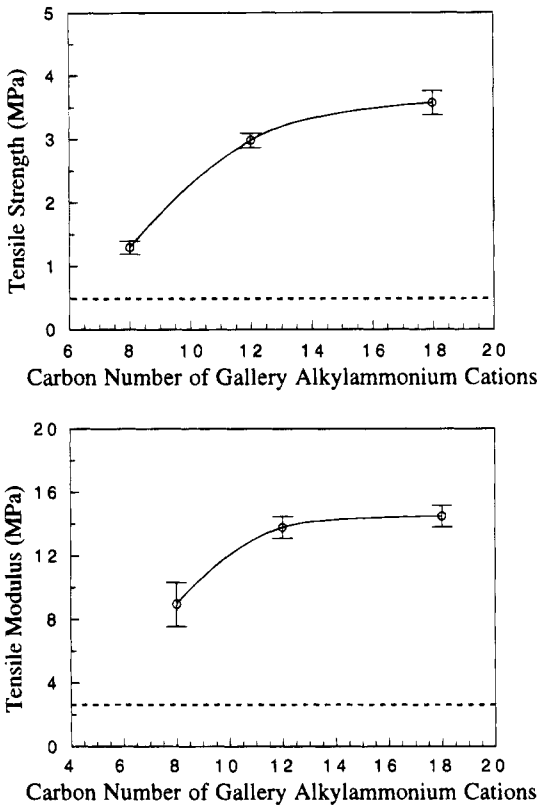

Figure 3. Dependence of tensile strength and modulus of epoxy–organoclay composites on the chain length of the clay-intercalated alkylammonium ions. The clay loading in each case was 10 wt %. The dashed lines indicate the tensile strength and modulus of the polymer in absence of clay.

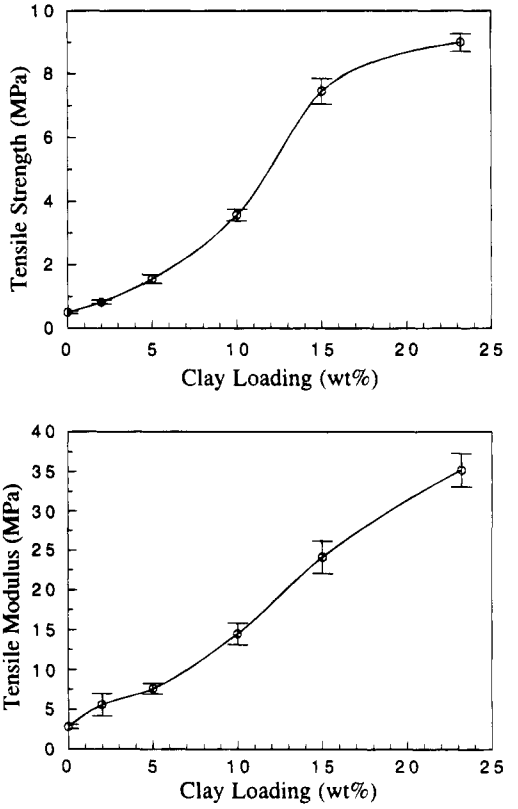

Figure 4. Dependence of tensile strength and modulus on clay loading for epoxy–$CH_3(CH_2)_{17}NH_3^+$–montmorillonite nanocomposites.

The tensile strengths and moduli of our new epoxy–clay nanocomposites have been measured according to the ASTM method 3039 using a UTS system. The relationship between the alkylammonium cation chain length of the organoclay and the mechanical properties of the composites is illustrated in Figure 3 for loadings of 10 wt % $CH_3(CH_2)_{n-1}NH_3^+$–montmorillonite. The presence of the organoclay substantially increases both the tensile strength and the modulus relative to the pristine polymer. The mechanical properties increase with increasing clay exfoliation in the order $CH_3(CH_2)_7NH_3^+$– < $CH_3(CH_2)_{11}NH_3^+$– < $CH_3(CH_2)_{17}NH_3^+$–montmorillonite. It is noteworthy that the strain at break for all of our epoxy–clay composites is essentially the same as the pristine matrix, suggesting that the exfoliated clay particles do not disrupt matrix continuity.

Reinforcement of the epoxy–clay nanocomposites also is dependent on clay loading. As shown in Figure 4, the tensile strength and modulus for the $CH_3(CH_2)_{17}NH_3^+$–montmorillonite system increases nearly linearly with clay loading. More than a 10-fold increase in strength and modulus is realized by the addition of only 15 wt % (~7.5 vol %) of the exfoliated organoclay.

In our previous studies[19, 20] of epoxide–*m*-phenylenediamine–clay nanocomposites, the tensile strength and modulus were marginally improved relative to the pristine polymer. In contrast, for the low-T_g epoxide–amine system of the present study, the reinforcement provided by the exfoliated clay is much more significant. Owing to the increased elasticity of the matrix above the T_g, the improvement in reinforcement may be due

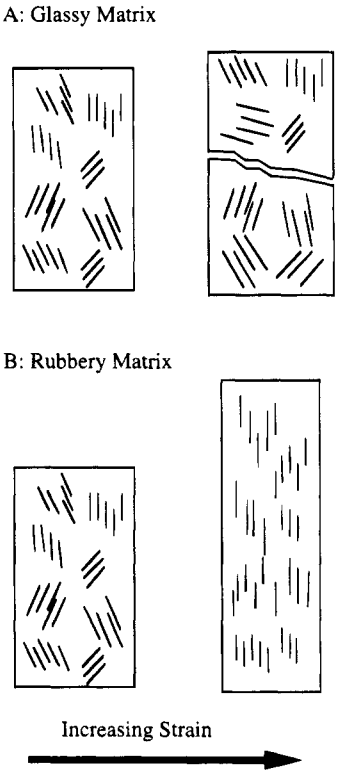

Figure 5. Proposed model for the fracture of (A) a glassy and (B) a rubbery polymer–clay exfoliated nanocomposite with increasing strain.

in large part to shear deformation and stress transfer to the platelet particles. In addition, platelet alignment under strain may also contribute to the improved performance of clays exfoliated in a rubbery matrix as

compared to a glassy matrix. The most significant difference between glassy and rubbery polymers is the elongation upon stress. The rubbery epoxy matrix used in this work exhibits 40–60% elongation at break, whereas for the glassy epoxy matrix we reported previously it is only 5–8%.[19,20] As illustrated in Figure 5, the clay platelets in the cured polymer will be partially aligned in the direction of the matrix surface. When strain is applied in the direction parallel to the surface, the clay layers will be aligned further. This strain-induced alignment of the layers will enhance the ability of the particles to function as the fibers in a fiber-reinforced plastics. Propagation of fracture across the polymer matrix containing aligned silicate layers is energy consuming, and the tensile strength and modulus are reinforced. In a glassy matrix, clay particle alignment upon applied strain is minimal and blocking of the fracture by the exfoliated clay is less efficient. Future X-ray scattering studies may provide direct evidence for the proposed contribution of clay particle alignment to composite reinforcement.

The discovery of substantial reinforcement by exfoliated clay particles in a rubbery epoxy polymer above T_g should advance the materials applications of these polymers. We are continuing to study the reinforcement mechanism by using smectite clays with complementary morphology and conducting modeling studies on the mechanical performance of the epoxy–clay exfoliated nanocomposites. The use of clay minerals as reinforcements in other rubbery materials, such as silicone rubber, and natural and synthetic rubbers also is being studied.

Acknowledgment. This research has been supported by the Michigan State University Center for Fundamental Materials Research and, in part, by the NSF under Grant CHE-92241023. We thank the MSU Composite Materials and Structures Center for the use of the UTS system for mechanical testing. This work also made use of the TEM facility in the MSU Center for Electron Optics.